Comparative Biochemistry and Physiology, Part B 198 (2016) 46–56

Contents lists available at ScienceDirect

Comparative Biochemistry and Physiology, Part B

journal homepage: www.elsevier.com/locate/cbpb

# Molecular characterization of two ferritins of the scallop *Argopecten purpuratus* and gene expressions in association with early development, immune response and growth rate

Teodoro Coba de la Peña [a,c,1], Claudia B. Cárcamo [a,b,1], María I. Díaz [a,b,d], Katherina B. Brokordt [a,b], Federico M. Winkler [a,b,*]

[a] Centro de Estudios Avanzados en Zonas Áridas (CEAZA), Universidad Católica del Norte, Larrondo 1281, Coquimbo, Chile
[b] Departamento de Biología Marina, Facultad de Ciencias del Mar, Universidad Católica del Norte, Larrondo 1281, Coquimbo, Chile
[c] Instituto de Ciencias Agrarias, Consejo Superior de Investigaciones Científicas (CSIC), Madrid, Spain
[d] Programa de Magíster en Ciencias del Mar mención Recursos Costeros, Facultad de Ciencias del Mar, Universidad Católica del Norte, Coquimbo, Chile

ARTICLE INFO

*Article history:*
Received 25 December 2015
Received in revised form 21 March 2016
Accepted 28 March 2016
Available online 01 April 2016

*Keywords:*
Ferritin
*Argopecten purpuratus*
Iron homoeostasis
Growth
Development
Immunity, Apfer1, Apfer2

ABSTRACT

Ferritin is involved in several iron homoeostasis processes in molluscs. We characterized two ferritin homologues and their expression patterns in association with early development, growth rate and immune response in the scallop *Argopecten purpuratus*, a species of economic importance for Chile and Peru. Two ferritin subunits (*Apfer1* and *Apfer2*) were cloned. *Apfer1* cDNA is a 792 bp clone containing a 516 bp open reading frame (ORF) that corresponds to a novel ferritin subunit in *A. purpuratus*. *Apfer2* cDNA is a 681 bp clone containing a 522 bp ORF that corresponds to a previously sequenced EST. A putative iron responsive element (IRE) was identified in the 5′-untranslated region of both genes. The deduced protein sequences of both cDNAs possessed the motifs and domains characteristic of functional ferritin subunits. Both genes showed differential expression patterns at tissue-specific and early development stage levels. *Apfer1* expression level increased 40-fold along larval developmental stages, decreasing markedly after larval settlement. *Apfer1* expression in mantle tissue was 2.8-fold higher in fast-growing than in slow-growing scallops. *Apfer1* increased 8-fold in haemocytes 24 h post-challenge with the bacterium *Vibrio splendidus*. *Apfer2* expression did not differ between fast- and slow-growing scallops or in response to bacterial challenge. These results suggest that *Apfer1* and *Apfer2* may be involved in iron storage, larval development and shell formation. *Apfer1* expression may additionally be involved in immune response against bacterial infections and also in growth; and thus would be a potential marker for immune capacity and for fast growth in *A. purpuratus*.



## 1. Introduction

Among bivalves, scallops are a valuable resource for fishing and aquaculture worldwide. The scallop *Argopecten purpuratus* is a species of importance for aquaculture in Chile and Peru. In Chile the production of this scallop species has relay on aquaculture for more than 30 years, since natural populations were decimated by overfishing (DiSalvo et al., 1984; Stotz and González, 1997). In recent years, cultured scallops have decreased their growth rates and experienced massive mortalities, in part due to pathogen infections. Therefore, the characterization of immune and growth proteins to be used as molecular markers of the health and growth status of *A. purpuratus* appears as an essential tool to support its culture. At present, immune-related genes have not been reported in the literature for *A. purpuratus*, and in general, despite its economic importance, little is known about the genetic factors that regulate its growth and immune capacity.

Ferritins are iron storage proteins that play a pivotal role in iron metabolism and homoeostasis of most organisms. Iron stored in ferritins is used to synthesize iron co-factors for respiration, photosynthesis, nitrogen fixation and DNA synthesis. Thus, ferritins have a central role in physiology and they are essentially ubiquitous (Theil, 1987; Harrison and Arosio, 1996; Arosio and Levi, 2010). In molluscs, ferritins have been functionally related to dietary iron (Wu et al., 2010), exposure to heavy metals (Zapata et al., 2009; Zhang et al., 2013b), antioxidation (He et al., 2011), thermal stress (Salinas-Clarot et al., 2011), development and shell formation (Wang et al., 2009; Huan et al., 2014), and recently to immune response to pathogen challenge (He et al., 2011; Kim et al., 2012; Li et al., 2012; Chávez-Mardones et al., 2013; Zhang et al., 2013a, 2013b).

Ferritins are molecular nanocages composed of 24 subunits (maxiferritins). Each subunit is a protein folded in 4-helical bundles, a fifth

* Corresponding author at: Departamento de Biología Marina, Facultad de Ciencias del Mar, Universidad Católica del Norte, Larrondo 1281, Coquimbo, Chile.
*E-mail address:* fwinkler@ucn.cl (F.M. Winkler).
[1] These authors contributed equally to the study.

http://dx.doi.org/10.1016/j.cbpb.2016.03.007
1096-4959/

short helix and a long extended loop (Crichton and Declercq, 2010). The ferritin shell surrounds a cavity containing an iron mineral core where thousands of iron atoms are stored (Harrison and Arosio, 1996; Le Brun et al., 2010). Ferritin subunits present in maxi-ferritin complexes have iron-binding sites with ferroxidase catalytic activity that bind two ferrous ions [Fe(II)] and oxidize them to ferric ions [Fe(III)]; using either dioxygen ($O_2$) or oxygen peroxide ($H_2O_2$) as oxidant co-substrate. The ferrihydrite nucleation centre, composed of several acidic residues on the inner cavity surface, facilitates the migration of the diferric oxo complex to the central cavity of the nanocage. In this way, ferric ions and oxygen atoms are stored by mineralization in the iron core (Harrison and Arosio, 1996; Liu and Theil, 2005; Liu et al., 2006). Thus, ferroxidase activity sequesters two Fenton reaction reagents, Fe(II) and $H_2O_2$, and the major cellular oxidant $O_2$, limiting free radical production and iron-mediated oxidative stress. Because of this, ferritins are considered to have an important antioxidant activity (Arosio et al., 2009).

In vertebrates, two major cytosolic ferritin subunit types have been characterized, named heavy (H) and light (L) chains. The H-ferritin subunit displays ferroxidase catalytic activity. The L-chain lacks a diiron binding site and ferroxidase activity, but contains the ferrihydrite nucleation centre, which facilitates iron storage (Harrison and Arosio, 1996; Arosio and Levi, 2010). A third type of cytosolic ferritin subunit, the M- (middle) type chain, has been identified in lower vertebrates that possesses both ferroxidase activity and an iron nucleation site (Giorgi et al., 2008; Arosio et al., 2009).

In animals, non-cytosolic ferritins have also been found in mammal and insect (*Drosophila melanogaster*) mitochondria (Galatro and Puntarulo, 2007; Arosio and Levi, 2010), and some secretory ferritins were found in certain invertebrates (Pham and Winzerling, 2010). Ferritin genes and functions have been poorly studied in marine invertebrates compared to vertebrates. However, cytosolic and secretory ferritins have already been identified in invertebrates, with differences in the number of homologous genes identified. Two H-type ferritins were identified in *Caenorhabditis elegans* (Dunkov and Georgieva, 2004). Also, an H-type ferritin was identified in the echinoderm *Asterias forbesi* (Beck et al., 2002). In molluscs, cytosolic and secretory H-type ferritins have been identified (He et al., 2011; Wang et al., 2009; Zhang et al., 2013a). For instance, two cytosolic and two secreted homologues were identified in *Crassostrea gigas* (Huan et al., 2014), and four cytosolic and two secretory ferritin homologues were identified in the scallop *Mizuhopecten yessoensis* (Zhang et al., 2013a; Sun et al., 2014).

Most known animal cytosolic ferritin mRNAs carry a *cis* non-coding regulatory element, the iron regulatory (or responsive) element (IRE), in the 5′ untranslated region (5′-UTR). IREs have a pivotal role in iron metabolism in animal cells. When intracellular iron concentration is low, a cytosolic repressor, the iron responsive protein (IRP), binds to the IRE hairpin structure at the 5′-UTR of ferritin mRNA and blocks ribosome binding and translation. When iron levels are high, IRPs are degraded or bind to other factors, and ferritin mRNA is efficiently translated (Theil, 1994; Finazzi and Arosio, 2014).

Different ferritin transcriptional regulators discovered in mammals included hormones, growth factors, inflammatory cytokines and second messengers, relating ferritin expression to stress, cell injury, altered cell regulation, and inflammation (Torti and Torti, 2002). In mammals, ferritins have been suggested also to be involved in apoptosis and immunomodulation (Recalcati et al., 2008). Vertebrate and invertebrate ferritins are also involved in innate immunity because of their iron-withholding ability (Ong et al., 2006). In the echinoderm *A. forbesi*, stimulated coelomocytes released iron into culture supernatants; upon stimulation by LPS, coelomocytes increased ferritin expression and the amount of iron in supernatants decreased over time, suggesting that ferritin could be an acute phase protein and is involved in iron sequestration (Beck et al., 2002). Simonsen et al. (2011) showed that a ferritin homologue was necessary for the full protective response of *C. elegans* against pathogenic bacteria by phenotypic characterization after RNAi knockdown of a ferritin gene.

The aim of the present study was to characterize *A. purpuratus* ferritin genes and their expression patterns in association with early development, immune response and growth rate; in order to assess their potential use as molecular marker for assisted *A. purpuratus* breeding programmes.

For this purpose, two ferritin subunit homologues were identified and characterized in *A. purpuratus*. Their cDNA sequences were studied and a phylogenetic analysis was carried out. Moreover, gene expression patterns were studied in different tissues, along larval development, in scallops challenged with pathogen bacteria, and in individuals with contrasting growth rates. Results suggest that one of these ferritin homologues, *Apfer1*, is a potential candidate gene to be used as a molecular marker for growth and immune response for assisted selection in breeding programmes for *A. purpuratus*.

## 2. Materials and methods

### 2.1. Ethical procedures

Animal maintenance and handling were carried out in strict accordance with the recommendations in the CCAC guidelines (http://www.ccac.ca/Documents/Standards/Guidelines). The protocol for sampling procedures and experimental manipulations was reviewed and approved by the Bioethics Committee of the Centro de Estudios Avanzados en Zonas Aridas (Permit Number: 005-13) and the National Council of Science and Technology of Chile.

### 2.2. Animals, challenge experiment and sample collection

*A. purpuratus* individuals were obtained from the farming centre of the Universidad Católica del Norte (Tongoy, Coquimbo, Chile, 30° 14′ S, 4004-M15 SERNAPESCA). Holding conditions are described in Pérez et al. (2009). A total of 15 adult individuals (14 months of age, 7–8 cm shell length) were collected and samples of several tissues (mantle, adductor muscle, gonads, gills and digestive gland) were extracted and fixed in RNA*later* Stabilization Reagent (Ambion Inc., Austin, Texas, USA) and stored at −80 °C for subsequent RNA purification.

Individuals at different stages of development were also collected. Adult scallops were induced to spawn (Pérez et al., 2009) and gametes were mixed together at concentrations sufficient to allow for fertilization. Three samples (i.e., biological replicates) of embryos (gastrulae; n = 1000 approx.), trochophores (n = 88 approx.), straight-hinged (veligers, n = 640 approx.), umbonal veligers (n = 500 approx.), pediveligers (n = 400 approx.) and juveniles (n = 300) were collected at 6 h, 24 h, 68 h, 8 d, 19 d and 23 d after fertilization, respectively. Each sample was centrifuged and immediately resuspended in RNA*later* and stored at −80 °C for subsequent RNA purification.

In order to compare gene expression in individuals in terms of contrasting growth rate, shell lengths and body weights of 350 four-month-old *A. purpuratus* individuals from a single reproduction batch were measured. From this batch, the 20 largest (25.25 ± 1.71 mm in shell length) and the 20 smallest (10.88 ± 0.65 mm in shell length) individuals were selected, and samples of mantle were individually obtained and preserved in RNA*later*. We chose the mantle tissue because it is involved in the shell formation process (Marin et al., 2008).

Challenge experiments were performed with the marine *V. splendidus* bacterium strain, reported as pathogenic for *A. purpuratus* larvae (Rojas et al., 2015). Bacteria were grown in trypticase soy broth (TSB) supplemented with 2% NaCl at 20 °C for 24 h. Subsequently, bacteria were inactivated by heating at 90 °C for 2 h and centrifuged at 14,500 *g* for 10 min. Supernatant was removed and the pellet was washed three times with sterile seawater. The pellet was then resuspended in sterile seawater at a final concentration of $10^7$ cells/mL. Forty *A. purpuratus* adult individuals were randomly divided into two groups. One group consisted of 20 individuals that were challenged by injection of 100 μL of the *V. splendidus* suspension ($10^7$ cells/mL) in the

adductor muscle with a 25 G syringe. The second group consisted of 20 individuals that were injected with 100 μL of sterile seawater and were used as controls. 1 mL of haemolymph from four individuals in each group was collected 2, 6, 12, 24 and 48 h after injection. There was an additional control group of four individuals that were not subjected to injection and from which haemolymph was collected at the time of injection of the individuals of the other groups, that is, at time 0 h. In order to avoid tank effects, control and treated individuals were placed at random into different pearl-nets in one 2000 L tank. Collected haemolymph samples were immediately centrifuged at 600 *g* at 4 °C for 10 min to harvest the haemocytes. Haemocytes were then immediately fixed in RNA*later* and stored at −80 °C.

All procedures with live scallops followed the recommendations of the EU Directive 2010/63/EU for animal experiments.

### 2.3. RNA extraction and first strand cDNA synthesis

Total RNA from each tissue and from whole larvae was extracted and treated with RNase-free DNase with an AxyPrep Multisource Total RNA Miniprep Kit (Axygen Biosciences, Union City, CA, USA). RNA from haemocyte pellets was extracted and treated with RNase-free DNase with the SV Total RNA Isolation System (Promega, Madison, WI, USA) according to the manufacturer's protocol. The RNA obtained was quantified with an Epoch spectrophotometer (BioTek, Winooski, VT, USA). RNA intactness was verified by visual inspection of integrity of 28S and 18S rRNA bands in denaturing formaldehyde/agarose gel electrophoresis stained with SYBR® Safe (Thermo Fisher Scientific). Each RNA sample was considered intact if 28S and 18S rRNA bands were sharp and discrete with an absence of smearing under either, and fluorescence intensity of 28S rRNA band appeared to be about twice as intense as the 18S rRNA band The RNA was stored at −80 °C for further use.

Reverse transcription (RT) of RNAs from tissues and larvae was carried out with a PrimeScript™ RT Reagent Kit with gDNA Eraser (TaKaRa, Japan) and oligo-p$(dT)_{15}$ primer. RT of RNA from haemocytes was carried out with an AffinityScript QPCR cDNA Synthesis Kit (Stratagene, Santa Clara, CA, USA) according to the manufacturer's protocol. RT of RNAs was done in equiproportions (i.e., from equal quantity of RNA) within all compared samples from each experiment.

### 2.4. Isolation of Apfer1 and Apfer2 full-length cDNAs

In order to isolate at less two different *A. purpuratus* ferritin homologues, two different pairs of oligonucleotides were used. The first primer pair, 5′-TCGTGAAACGCTACCACCTA-3′ (forward) and 5′-CTTCACATTT TATTTCCCTGTCA-3′ (reverse), was designed from the sequence of *Argopecten irradians* ferritin 1 (*Aifer1*, GenBank Acc. No. HQ225739).

cDNA from mantle tissue of *A. purpuratus* adult individuals (14 months of age) was used for PCR. PCR reaction contained 5 μL of cDNA and 0.2 μM (final concentration) of each primer, in a final volume of 20 μL. The initial denaturing time was 3 min, followed by 30 PCR cycles of 94 °C, 40 s; 60 °C, 40 s; and 72 °C, 40 s. A 624-bp PCR product was obtained, purified and sequenced by the Sequencing Service of the Pontificia Universidad Católica de Chile. In order to obtain the 5′ untranslated region (5′-UTR), 5′-RACE (rapid amplification of cDNA ends)-Ready cDNA was obtained with a SMARTer™ RACE cDNA Amplification Kit (Clontech, Palo Alto, CA, USA) and primer 5′-CTGACGGCCA TTTTGACGTTTTAGGTGG-3′. Thermal cycling parameters were set in accordance with the manufacturer's instructions. The amplification product was visualized on agarose gels, purified, and ligated into pGEM-T Easy vector (Promega, Madison, WI, USA). Subsequently, competent cells of *Escherichia coli* JM-109 (Promega) were transformed with the plasmid by heat shock and then cultured in agar plates LB/Amp/IPTG/X-gal overnight at 37 °C. Plasmids containing the insert were purified with an E.Z.N.A. Plasmid DNA Mini kit (OMEGA Biotek, Norcross, GA, USA). The resulting cDNA was sequenced, and the sequences of the 624-bp PCR and 5′-RACE products were aligned at the overlapping regions to produce a full-length cDNA sequence.

In order to obtain a second *A. purpuratus* ferritin homologue, a second primer pair was designed from the published sequence of a ferritin EST form *A. purpuratus* (GenBank ES469340; Boutet et al., 2008) that is homologous to *Aifer2* of *A. irradians* (GenBank HQ225741). Primers were: 5′-GTGAACGTACGGGCAAAGTT-3′ (forward) and 5′-TTCTGGGC TAAATGTATCAACA-3′ (reverse), PCR was performed with these primers under the same conditions described above, and generated a 681-bp PCR product that was cloned and sequenced as described above.

### 2.5. Sequence analyses

Sequences were analysed by BLAST (http://blast.ncbi.nlm.nih.gov/) and the Expert Protein Analysis System (http://web.expasy.org/). Sequences were translated into predicted amino acid sequences, and both nucleotide and predicted protein sequences were aligned with various known ferritin sequences with the ClustalW Multiple Sequence Alignment programme (http://www.ebi.ac.uk/Tools/msa/clustalw2/). The iron responsive elements (IREs) and stem-loop structures of the two ferritin gene homologues were predicted by the SIREs Web Server v2.0 (http://ccbg.imppc.org/sires/) (Campillos et al., 2010). The tertiary structures of deduced proteins codified by *Apfer1* and *Apfer2* were predicted through the I-TASSER (Iterative Threading ASSEmbly Refinement) server (http://zhanglab.ccmb.med.umich.edu/I-TASSER/) (Zhang, 2008). The resultant theoretical model proteins were displayed and analysed with PyMOL software (Schrödinger, 2010).

A phylogenetic analysis was performed with MEGA software v6.06 (Tamura et al., 2013) using the neighbour-joining method (Saitou and Nei, 1987). The evolutionary distances were computed with the maximum composite likelihood method (Tamura et al., 2004). Node robustness was assessed by the bootstrap method ($N = 2000$ pseudo-replicates).

### 2.6. Quantitative real-time PCR

Primers for real-time PCR reaction were designed with Primer Express v3.0 software (Applied Biosystems, Foster City, CA, USA) to have melting temperatures of 58 to 60 °C and generate PCR products of 50 to 150 bp. β-actin was used as endogenous control in order to normalize experimental results (Zapata et al., 2009). In order to validate β-actin as a housekeeping gene for our samples, statistical tests on β-actin expression values among different tissues, developmental stages or challenged animals were performed, and non-significant differences were found among them ($P > 0.05$). Primer sequences were as follows: *Apfer1* (forward, 5′-CATCACCAACCTGAAACGTGTT-3′; reverse, 5′-TACTCCAG GGATTCTTTGTCGTACA-3′); *Apfer2* (forward, 5′-CGACAAGGAGTCCATC AATGG-3′; reverse, 5′-AATGTATCAACACTGCCAGAAGCT-3′); β-actin (forward, 5′-GAATCTGGCCCATCCATTGT-3′; reverse, 5′- CGTTCTCGTG GATTTTTTTCAAGT-3′).

Each PCR reaction contained 10 μL 2× Maxima® SYBR Green/ROX qPCR Master Mix (Thermo Scientific, Rockford, IL, USA), 2 μL cDNA and 0.3 μM (final concentration) of each primer, in a final volume of 20 μL. Minus-reverse transcriptase (−RT) controls of the RNA samples were included in real-time RT-PCR experiments, in order to detect and estimate genomic DNA contamination. Genomic DNA contamination was considered negligible whether $\Delta C_T$ between –RT and + RT samples was ≥10 (Laurell et al., 2012). Real-time PCR reactions were run in an Eco Real-Time PCR System (Illumina, San Diego, CA, USA). Initial denaturation time was 10 min at 95 °C, followed by 40 PCR cycles of 95 °C, 15 s and 60 °C, 1 min. After the PCR cycles, the purity of the PCR product was checked by the analysis of its melting curve; the thermal profile for melting curve analysis consisted of denaturation for 15 s at 95 °C, lowered to 55 °C for 15 s and then increased to 95 °C for 15 s with continuous fluorescence readings. By serial dilution of cDNA, RT-qPCR efficiency was set to be between 95 and 110%. Efficiency of *Apfer1* gene

amplification was not similar to that of the housekeeping gene (as it was determined by slope calculation), so the standard curve method was applied for relative quantification of *Apfer1*. Efficiency of *Apfer2* amplification was similar to that of the housekeeping gene, so the comparative $C_T$ method (also called the $\Delta\Delta C_T$ method; Pfaffl, 2001) was applied for relative quantification of *Apfer2*. Experiments included five biological replicates except in larvae expression (three biological replicates), and three technical replicates were performed. Mean values ± SE were presented.

### 2.7. Statistical analyses

Data were analysed with the STATISTICA v7.0 software package (StatSoft Inc., Tulsa, OK, USA). The following statistical tests were performed: one-way analysis of variance (one-way ANOVA) and Tukey post-hoc test for data of gene expression in tissues and larvae; *t*-test of the differences between two means for data of gene expression in small and large individuals; data of gene expression upon bacterial challenge were analysed by factorial ANOVA (in order to assess the effect of two factors: presence or absence of bacteria and time post-challenge) and Tukey post-hoc test. We applied a sequential Bonferroni procedure to correct for type I error in multiple simultaneous tests. Differences were considered significant at $P < 0.05$. For ANOVAs, normality of the dependent variable was tested with the Shapiro–Wilks test (SAS Institute, 1999) and homogeneity of variances with the Levene test (Snedecor and Cochran, 1989) to verify that the data met model assumptions.

## 3. Results and discussion

### 3.1. cDNA cloning, sequence characterization of Apfer1 and Apfer2

Two full-length clones were isolated from mantle of *A. purpuratus*. The full-length cDNA clones were designated as *Apfer1* (for *A. purpuratus* ferritin 1) and *Apfer2*, and they were 792 and 681 bp length, respectively. The open reading frames (ORFs) of both genes were 516 and 522 bp length, encoding 171 and 173 amino acids, respectively. The predicted molecular weights of the deduced proteins coded by *Apfer1* and *Apfer2* were 19.68 and 19.87 kDa and the theoretical isoelectric points (pI) were 4.97 and 4.96, respectively. Both predicted proteins contained an iron binding region signature (IBRS, 59EEREHAEKFMKYQNKRGGR77) and seven conserved residues (E25, Y32, E59, E60, H63, E105, Q139) of the ferroxidase diiron centre, which catalyses Fe(II) oxidation in mammalian H ferritins (Fig. 1A and B). Four conserved negatively charged amino acids (K55, D58, E59, E62) are known to promote ferrihydrite nucleation in mammalian L-type subunits. A potential bio-mineralization residue (Y27) and three conserved ion channel amino acids (H116, D129, E132) that facilitate access of iron ions to the ferritin protein were also identified. Proteins coded by *Apfer1* and *Apfer2* have seven (Y38, S57, T93, S111, S125,

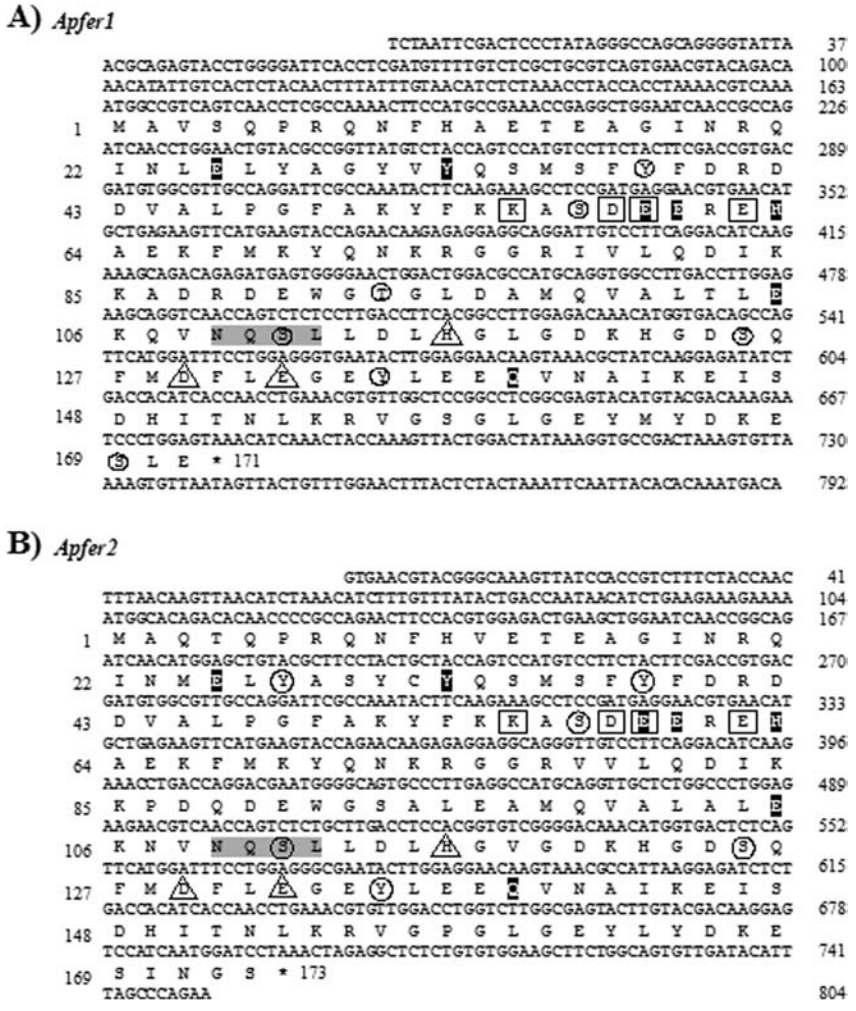


**Fig. 1.** Nucleotide and deduced amino acid sequences of *Apfer1* (A) and *Apfer2* (B) from *Argopecten purpuratus*. Methionine (M) at position 1 of the protein is codified by the start codon (ATG); asterisk denotes the stop codon (TAA). IRE sequences are single underlined. Conserved residues for the ferroxidase site are shaded in black. Conserved residues of the ferrihydrite nucleation centre are contained in square boxes. Conserved ion channel amino acids are contained in triangles. Conserved amino acids with putative phosphorylation sites are contained in circles. Putative N-glycosilation site (NQSL) is shaded in dark grey.

Y135, S169) and six (Y27, Y38, S57, S111, S125, Y135) amino acids with putative phosphorylation sites, respectively. In addition, a putative N-glycosylation site (109NQSL112), which is present in many ferritins, was found in both amino acid sequences (Fig. 1A and B). Thus, *Apfer1* and *Apfer2* presented all sequence motifs determining ferritin function (Theil, 1987; Harrison and Arosio, 1996). As M-type ferritins, they have both the ferroxidase activity characteristic of H-type ferritins and the iron nucleation site observed in L-type ferritins (Arosio et al., 2009). No putative signal peptide was detected, which suggested that both predicted ferritins are cytosolic proteins.

Pairwise and multiple alignment of nucleotide and protein sequences showed that *Apfer1* and *Apfer2* displayed high nucleotide and amino acid identities with other mollusc and invertebrate ferritin homologues. *Apfer1* corresponded to a new ferritin homologous sequence (GenBank accession no. KT895278) and showed 97% nucleotide identity (99% amino acid identity) with *A. irradians* ferritin 1 (GenBank accession no. HQ225739). *Apfer2* (GenBank accession no. KT895279) corresponded to a partial sequence of an EST (GenBank accession no. ES469340) obtained from a cDNA library from gonad tissue of *A. purpuratus* (Boutet et al., 2008). *Apfer2* showed 87% nucleotide identity (99% amino acid identity) with *A. irradians* ferritin 2 (GenBank: GU263464). *Apfer1* showed 88% nucleotide identity (89% amino acid identity) with *Apfer2*. Apfer1 and Apfer2 showed high amino acidic identities with other mollusc sequences (Fig. 2). *A. purpuratus* ferritins 1 and 2 display considerable homologies with H and M ferritin subunits of vertebrates, and to a lesser extent with ferritin L subunits.

The potential 3D models of the tertiary structures of Apfer1 and Apfer2 were generated by the I-TASSER server, using multiple threading approaches and iterative template fragment assembly simulations (Fig. 3A and B). The proteins from the protein data bank (PDB) that

```
Apfer1           M---AVS-QP RQNFHAETEA GINRQINLEL YAGYVYQSMS FYFDRDDVAL   46
A. irradians 1   M---AVS-QP RQNFHAETEA GINRQINLEL YAGYVYQSMS FYFDRDDVAL   46
Apfer2           M---AQT-QP RQNFHVETEA GINRQINMEL YASYCYQSMS FYFDRDDVAL   46
A. irradians 2   M---AQT-QP RQNFHVETEA GINRQINMEL YASYCYQSMS FYFDRDDVAL   46
H. diversicolor  M---ANT-QP RQNFHVESEA GINRQINMEL YASYTYQSIA FYFDRDDVAL   46
C. gigas         M---SQS-QP RQNFHEESEA GINRQINMEL YASYTYQSMA LYFDRDDVAL   46
R. mioroplus     M---AAT-QP RQNYHVDCEA RINKQINLEL YASYVYTSMA YYFDRDDVAL   46
D. rerio (H)     M----DS-QV RQNYDRDCEA LINKMINLEL YAGYTYTSMA FYFDRDDVAL   45
D. rerio (M)     M----ETCQI RQNYDRDCEA AINKMINLEL YAGYTYTSMA HYFKRDDVAL   46
X. laevis        M----QS-QV RQNFHSDCEA AINRMVNMEM YASYVYLSMS YYFDRDDVAL   45
C. milii         M----TS-QV RQNYHQECEA AINRQVNIEL YASYTYLSMS YYFDRDDVAL   45
H. sapiens (H)   MTTASTS-QV RQNYHQDSEA AINRQINLEL YASYVYLSMS YYFDRDDVAL   49
H. sapiens (L)   M----SS-QI RQNYSTDVEA AVNSLVNLYL QASYTYLSLG FYFDRDDVAL   45

Apfer1           PGFAKYFKKA SDEEREHAEK FMKYQNKRGG RIVLQDIKKA DRDEWGTGLD   96
A. irradians 1   PGFAKYFKKA SDEEREHAEK FMKYQNKRGG RVVLQDIKKA DRDEWGTGLD   96
Apfer2           PGFAKYFKKA SDEEREHAEK FMKYQNKRGG RVVLQDIKKP DQDEWGSALE   96
A. irradians 2   PGFAKYFKKA SDEEREHAEK FMKYQNKRGG RVVLQDIKKP DQDEWGSALE   96
H. diversicolor  PGFSKYFKKA SEEEREHAEK LMKYQNTRGG RIVLQDIKKP DRDEWGSALE   96
C. gigas         PGFHKFFKHS SDEEREHAEK LMKYQNKRGG RIVLQDIKKP DRDEWGTGLD   96
R. mioroplus     PGFHKFFKKS SDEEREHAQK LMKYQNMRGG RVVLQAIQKP SRDEWGAGLD   96
D. rerio (H)     PGFAKFFKKN SEEEREHAEK FMEFQNKRGG RIVLQDIKKP ERDEWDNGLT   95
D. rerio (M)     PGFAKFFNKN SEEEREHAEK FMEFQNKRGG RIVLQDIKKP DRDVWGNGLI   96
X. laevis        HHVAKFFKEQ SHEEREHAEK FLTYQNKRGG RVVLQDIKKP ERDEWGNTLE   95
C. milii         KNFAKFFKEQ SHEEQEHAER LLKYQNQRGG RINLLDIKKA DQNIWGNGLE   95
H. sapiens (H)   KNFAKYFLHQ SHEEREHAEK LMKLQNQRGG RIFLQDIKKP DCDDWESGLN   99
H. sapiens (L)   EGVSHFFREL AEEKREGYER LLKMQNQRGG RALFQDIKKP AEDEWGKTPD   95

Apfer1           AMQVALTLEK QVNQSLLDLH GLGDKHGDSQ FMDFLEGEYL EEQVNAIKEI  146
A. irradians 1   AMQVALTLEK QVNQSLLDLH GLGDKHGDSQ FMDFLEGEYL EEQVNAIKEI  146
Apfer2           AMQVALALEK NVNQSLLDLH GVGDKHGDSQ FMDFLEGEYL EEQVNAIKEI  146
A. irradians 2   AMQVALALEK NVNQSLLDLH GVGDKHGDAQ FQDFLESEYL EEQVNAIKEI  146
H. diversicolor  SMQVALSLEK NVNQALLDLH AVASKHNDAQ MCDFLESEYL EEQVKAIKEI  146
C. gigas         AMQIALQLEK SVNQSLLDLH KLADGHRDAQ MCDFIESEFL EEQVNAIKEI  146
R. mioroplus     AMQAALELEK TVNQSLLDLH KLANDHNDAQ LCDFLESEYL EEQVKAIKEL  146
D. rerio (H)     AMQCALQLEK NVNQALLDLH KVASQKGDPH LCDFLESHYL NEQVEAIKKL  145
D. rerio (M)     AMQCALQLEK NVNQALLDLH KLATEMGDPH LCDFLESHYL DEQVEAIKKL  146
X. laevis        AMQAALQLEK TVNQALLDLH KLGSDKVDPH LCDFLESEYL EEQVKAMKQL  145
C. milii         AMQFALNLEK SVNQSLLDLH NLASTHNDPQ LCNFLETHYL DEQVEAIKKL  145
H. sapiens (H)   AMECALHLEK NVNQSLLEIH KLATDKNDPH LCDFIETHYL NEQVKAIKEL  149
H. sapiens (L)   AMKAAMTLEK KLNQALLDLH ALGSARTDPH LCDFLETHFL DEEVKLIKKM  145

Apfer1           SDHITNLKRV GS---GLGEY MYDKESL--- ---E  171
A. irradians 1   SDHITNLKRV GS---GLGEY LYDKESL--- ---E  171
Apfer2           SDHITNLKRV GP---GLGEY LYDKESING- ---S  173
A. irradians 2   SDHITNLKRV GP---GLGEY LYDKESING- ---S  173
H. diversicolor  SDHITNLKRV GT---GLGEY MYDKESM--- ---E  171
C. gigas         SDHVTQLKRV GA---GLGEY QYDKQLQ--- ---S  171
R. mioroplus     SDYVTNLKRV GP---GLGEY MFDKETLS-- ---D  172
D. rerio (H)     GDHITNLSKM DAGNNRMAEY LFDKHTLD-- ---S  174
D. rerio (M)     GDHITNLSKM DAGNNRMAEY LFDKQTLD-- ---S  175
X. laevis        GDYITNLKRL GVPQNGMGEY LFDKHTLGES ---S  176
C. milii         GDHISNLIRL GVPSNGMGEY LFDKLTLNES ---G  176
H. sapiens (H)   GDHVTNLRKM GAPESGLAEY LFDKHTLGDS DNES  183
H. sapiens (L)   GDHLTNLHRL GGPEAGLGEY LFERLTLKH- ---D  175
```

**Fig. 2.** Multiple sequence alignment of vertebrate and invertebrate ferritin subunits. Conserved residues, important in iron binding and ferroxidation, are shaded in light grey. A conserved Y residue involved in biomineralization of iron is shaded in dark grey. Ferritin sequences shown are from: *Argopecten purpuratus* (Apfer1; Apfer2); *A. irradians* 1 (GenBank: AEN71558) and 2 (GenBank: ADR71732); *Haliotis diversicolor* (GenBank: ABY87353); *Crassostrea gigas* (soma ferritin-like; GenBank: XP_011432947); *Rhipicephalus microplus* (GenBank: AAQ54710); *Danio rerio* heavy (H; GenBank: NP_001002378) and middle (M; GenBank: XP_687175) chain; *Xenopus laevis* heavy chain 1 (GenBank: NP_001090207); *Callorhinchus milii* mitochondrial subunits (GenBank: AFM87250); *Homo sapiens* heavy (H; GenBank: NP_002023) and light (L; GenBank: AAA35831) subunits.

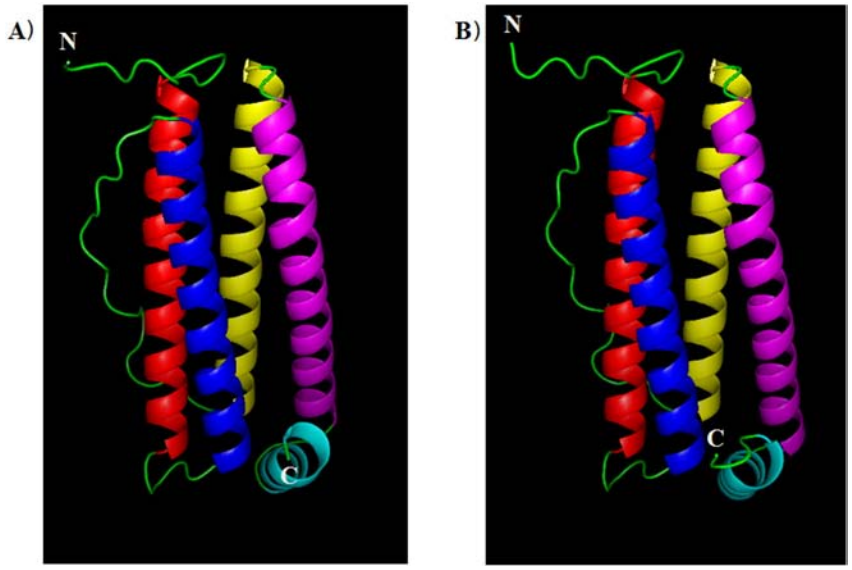


**Fig. 3.** Predicted 3D structural models of Apfer1 (A) and Apfer2 (B) subunits from *Argopecten purpuratus*. The four α helixes are coloured in red, blue, yellow and magenta. A fifth short helix is coloured in cyan. Random coils and turns are coloured in green. N, N-terminal; C, C-terminal. (For interpretation of the references to colour in this figure legend, the reader is referred to the web version of this article.)

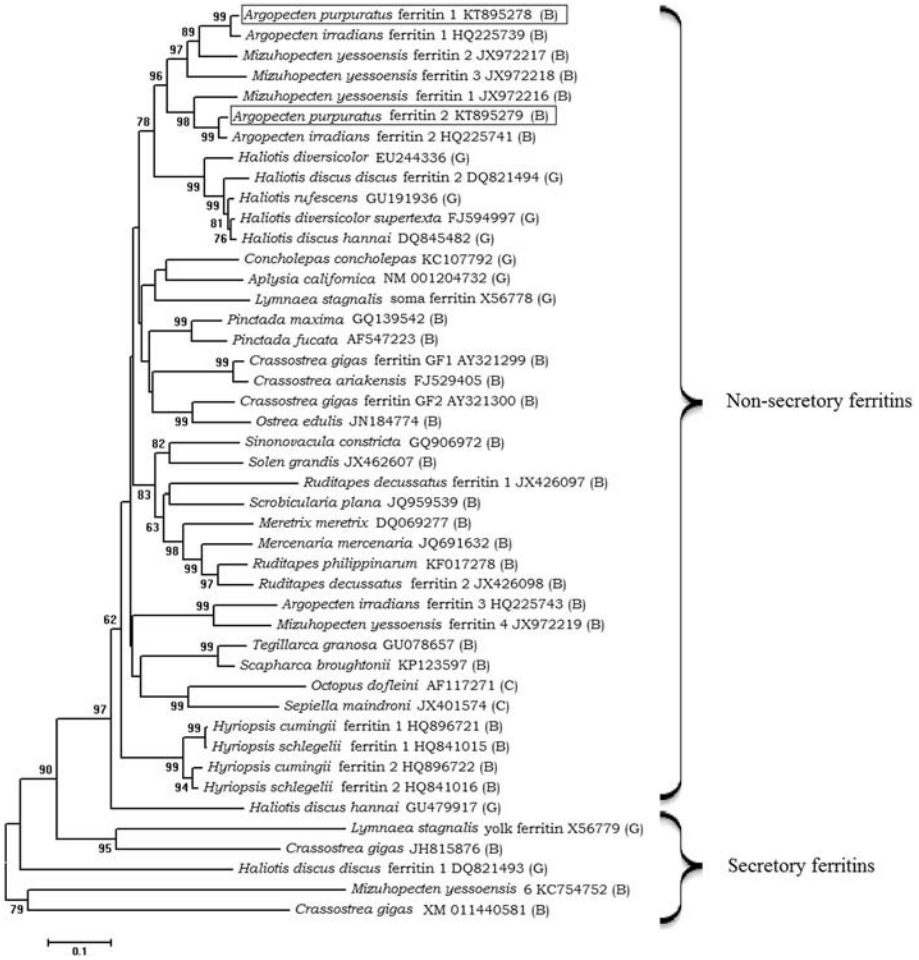


**Fig. 4.** Phylogenetic optimal tree of most known nucleotide coding sequences of mollusc ferritin. Subunits *Apfer1* and *Apfer2* references are contained in boxes. The evolutionary history was inferred from the neighbour-joining method. Bootstrap values are shown next to the branches. The tree is drawn to scale, with branch lengths in the same units as those of the evolutionary distances used to infer the phylogenetic tree. (B), Class Bivalvia; (C), Class Cephalopoda; (G), Class Gastropoda. GeneBank accession numbers are indicated.

have the closest structural similarity to the predicted I-TASSER models for Apfer1 and Apfer2 were the human heavy chain ferritin (PDB: 2CN7) and a frog M ferritin (PDB: 3KA3), respectively. Apfer1 and Apfer2 3D models consisted of four α helixes from the N-terminal that were parallel with each other, binding together through random coils and turns (Fig. 3A and B). A fifth short C-terminal α helix was also present in both Apfer1 and Apfer2. Thus, predicted 3D models of Apfer1 and Apfer2 resembled the typical spatial features of known H- and M-type

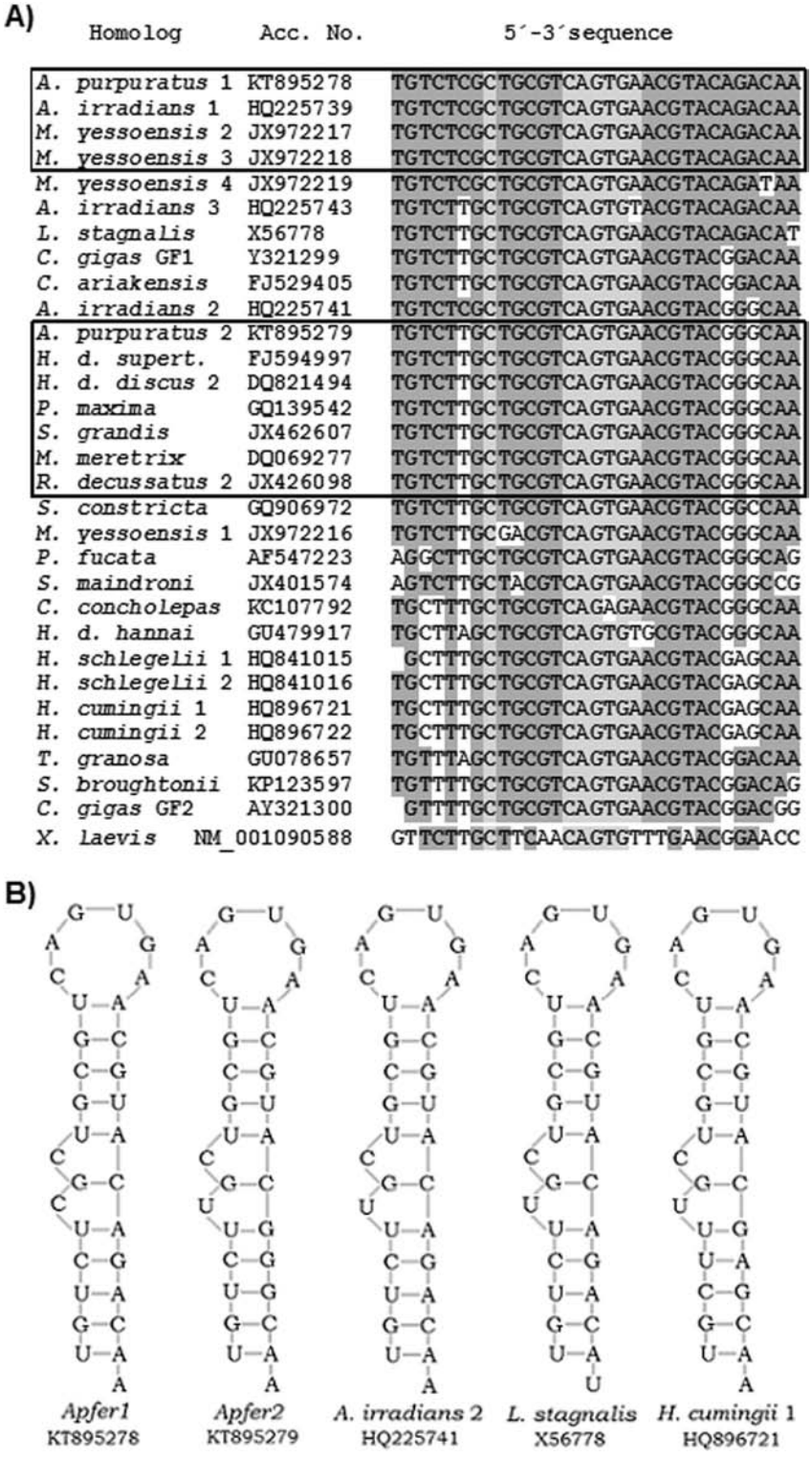


**Fig. 5.** Iron responsive element (IRE) sequences and stem-loop structures of the two ferritin gene homologues. (A) Alignment and sequence comparison of most known iron responsive elements (IREs) from mollusc ferritin subunits (and of the non-molluscan ferritin of *Xenopus laevis*). Sequence of IRE of *Apfer1*, complete IRE sequence corresponding to *Apfer2* (full IRE sequence: GenBank: ES469340) of *Argopecten purpuratus* and respective identical IRE sequences of other mollusc species are contained in boxes. Acc. No of each ferritin homologue is indicated. Conserved 5′-CAGTGN-3′ loop structure residues and bulged cysteines located five bases upstream are shaded in light grey. The other homologous regions are shaded in dark grey. Sequence of IRE of *Apfer1* was used as reference. (B) Predicted IRE stem-loop structures of *Apfer1* and IRE corresponding to *Apfer2* (GenBank: ES469340) compared with IREs of *A. irradians* 2 (GenBank: HQ225741), *L. stagnalis* (GenBank: X56778) and *H. cumingii* 1 (GenBank: HQ896721). The conserved 5′-CAGTGN-3′ loop structure residues and the conserved bulged C are shaded in grey.

ferritin structures (Harrison and Arosio, 1996; Crichton and Declercq, 2010).

Phylogenetic analysis of *Apfer1* and *Apfer2* revealed two clades, one including the non-secretory (40 nucleotide coding sequences) and the other the secretory (five nucleotide coding sequences) subunits (Fig. 4). The non-secretory clade included *Apfer1*, *Apfer2* and most other known molluscan ferritin subunits. Clades including *Apfer1* and *Apfer2* further clustered together, and formed a clade with ferritin subunits of several *Haliotis* species (bootstrap values >70; Fig. 4).

Analysis of the 5′-UTR demonstrated the presence of a putative iron responsive element (IRE) in the *Apfer1* cDNA clone. A partial IRE sequence was found in the 5′-UTR of *Apfer2*; a BLAST search allowed identification of the corresponding complete IRE sequence for the *Apfer2* gene in an *A. purpuratus* gonad library (EST66, GenBank: ES469340; Boutet et al., 2008) (Fig. 5A). IRE of *Apfer1* and IRE corresponding to *Apfer2* are predicted to be folded into a typical stem-loop secondary structure, which perfectly matches all IRE characteristics, including a conserved six nucleotide loop 5′-CAGUGN-3′ and a bulged C located five bases upstream of this loop (Fig. 5B). IREs are important regulatory elements as binding sites for IBPs and Fe(II) (Theil, 2015), suggesting that *Apfer1* and *Apfer2* syntheses are probably postranscriptionally regulated by iron.

The comparison of the ferritin coding sequences of the phylogenetic tree with their corresponding IRE sequences show that *Apfer1* and the other three ferritin homologues of its clade displayed the same IRE sequence (Figs. 4 and 5A), suggesting that these coding sequences and their IREs had experienced similar molecular evolution events. However, the *Apfer2* shared its IRE sequence with less-related clades (Figs. 4 and 5A). It has been reported that IRE sequences are highly conserved within taxonomic groups, and evolve through stepwise changes in sequence, rather than by recombination events (Piccninelli and Samuelsson, 2007). Our results suggest that the evolutionary history of some ferritin IRE sequences can differ from that of their corresponding coding sequences. Further characterization and phylogenetic analysis of new homologues and more detailed studies on function and regulation mechanisms between ferritin homologues will shed light on the molecular evolution of ferritins in molluscs.

### 3.2. Tissue-specific mRNA levels of Apfer1 and Apfer2

Tissue-specific expression patterns of *Apfer1* and *Apfer2* were analysed in different organs of adult individuals, including gill, adductor muscle, mantle, gonad and digestive gland. *Apfer1* and *Apfer2* transcripts were detectable in all the examined tissues (Fig. 6). *Apfer1* was most strongly expressed in the digestive gland (mean expression ± SE: 1,493 ± 595) (Fig. 6A), and the lowest expression was observed in mantle and gills (1.0 ± 0.3 and 0.9 ± 0.23, respectively). A high ferritin expression in the digestive gland was also observed in other molluscs such as *Pinctada fucata* (Zhang et al., 2003), *C. gigas* (Durand et al., 2004), *Haliotis discus discus* (De Zoysa and Lee, 2007), *Haliotis rufescens* (Salinas-Clarot et al., 2011) and *Haliotis diversicolor supertexta* (Xie et al., 2012). The digestive gland in molluscs is the main centre for metabolic regulation, participating in the mechanisms of immune defence and homoeostatic regulation of the internal medium, and is a major site for metal accumulation and iron storage (Marigómez et al., 2002). Thus, *Apfer1* may be highly specific for iron storage in digestive glands.

The highest level of *Apfer2* mRNA was observed in adductor muscle (7.3 ± 2.5), being lower in other tissues, as digestive gland and gills (4.2 ± 0.61 and 1.05 ± 0.14, respectively) (Fig. 6B). Adductor muscle is the most important locomotion organ in molluscs, especially scallops; therefore, ferritins expressed in this tissue may be putatively involved in iron storage and energy metabolism (He et al., 2011). Functional characterization of both genes will shed light on their physiological roles in organs.

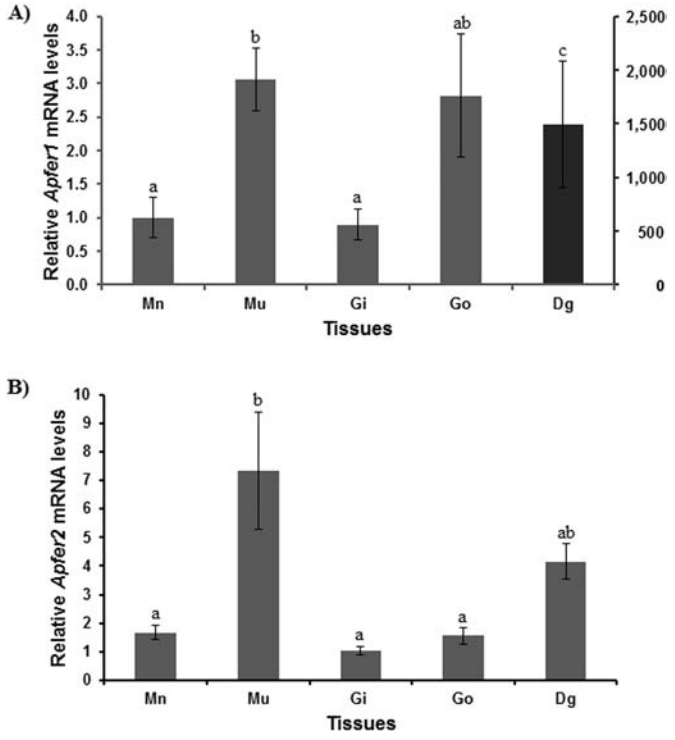


**Fig. 6.** Relative levels of *Apfer1* (A) and *Apfer2* (B) mRNA transcripts in different tissues of adult of *Argopecten purpuratus*. Transcript levels of *Apfer1* and *Apfer2* in mantle (Mn), adductor muscle (Mu), gill (Gi), gonad (Go) and digestive gland (Dg) were detected by real-time PCR. Relative expression in mantle was used as reference. β-actin was used as housekeeping gene. In figure A, gene expression level in digestive gland (dark grey bar) corresponds to the vertical scale on the right. All values represent the means ± S.E. (n = 5 biological replicates). Different letters denote $P < 0.05$.

### 3.3. Apfer1 and Apfer2 expression in different developmental stages

It has been suggested that ferritin is involved in mollusc shell formation by controlling the distribution of iron, which induces calcification in the mantle tissue, a critical event for shell development (Zhang et al., 2003; Wang et al., 2009; Zhang et al., 2013a; Huan et al., 2014). Shell formation begins during larval development, and in bivalves the first shell is secreted during the trochophore stage (Marin et al., 2008). Our results showed marked changes in expression patterns of *Apfer1* and *Apfer2* during larval development of *A. purpuratus* (Fig. 7). It was observed that *Apfer1* expression level increased along the different developmental stages (about 40-fold), from embryos (mean expression ± SE: 1.0 ± 0.3) to the premetamorphic stage (i.e., pediveliger, 39.7 ± 17). Significant highest expression levels were observed in veligers (29.8 ± 3.3) and pediveligers. However, a significant drop in expression was observed in the subsequent juvenile stage (8.2 ± 0.98) (Fig. 7A), suggesting that this ferritin homologue may be involved in prodissoconch I and prodissoconch II shell formation during the first larval stages up to the metamorphosis of the veliger larva.

In contrast, the highest *Apfer2* expression levels were observed in the gastrula stage (mean expression ± SE: 1.21 ± 0.05) (Fig. 7B) and this may be related to the formation of the shell field. A significant drop in expression was observed in the subsequent stages. After trocophore and straight veliger development, a significant increase in gene expression was observed at veliger and pediveliger stage, followed by a significant decrease in *Apfer2* expression in juveniles (0.47 ± 0.08 and 0.49 ± 0.02, respectively) (Fig. 7B). *Apfer2* expression pattern from trocophore to juvenile stage is similar to that observed in *Apfer1*. Thus, both genes could be involved in larval development and shell formation.

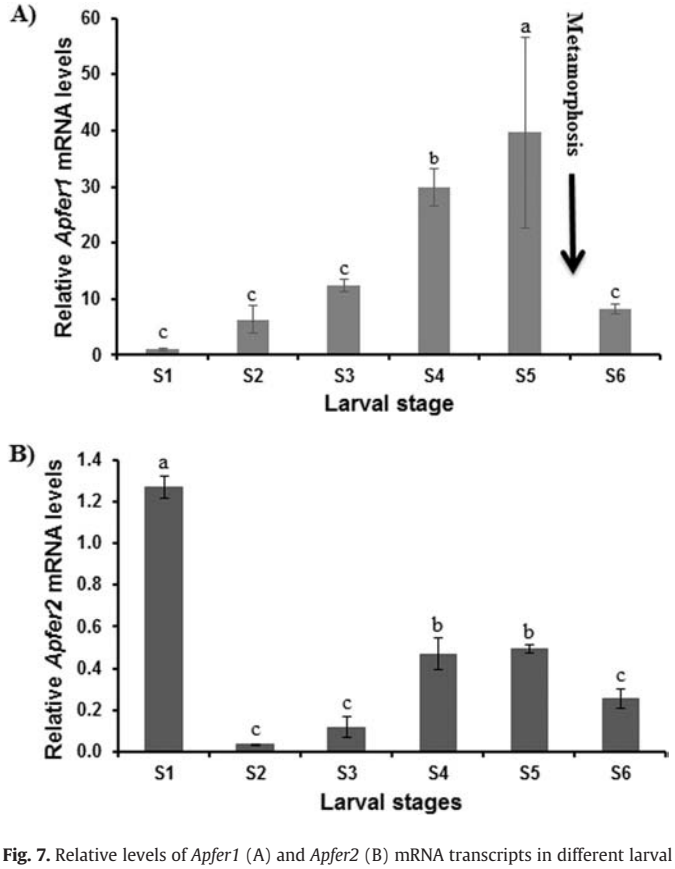


**Fig. 7.** Relative levels of *Apfer1* (A) and *Apfer2* (B) mRNA transcripts in different larval stages of *Argopecten purpuratus*. S1, embryos (gastrulae); S2, trochophores; S3, straight-hinged (veligers); S4, umbonal veligers; S5, pediveligers; S6, juveniles. Metamorphosis stage is indicated by an arrow. All values represent the means ± S.E. (n = 3 biological replicates of larvae/juvenile pools). Different letters denote $P < 0.05$.

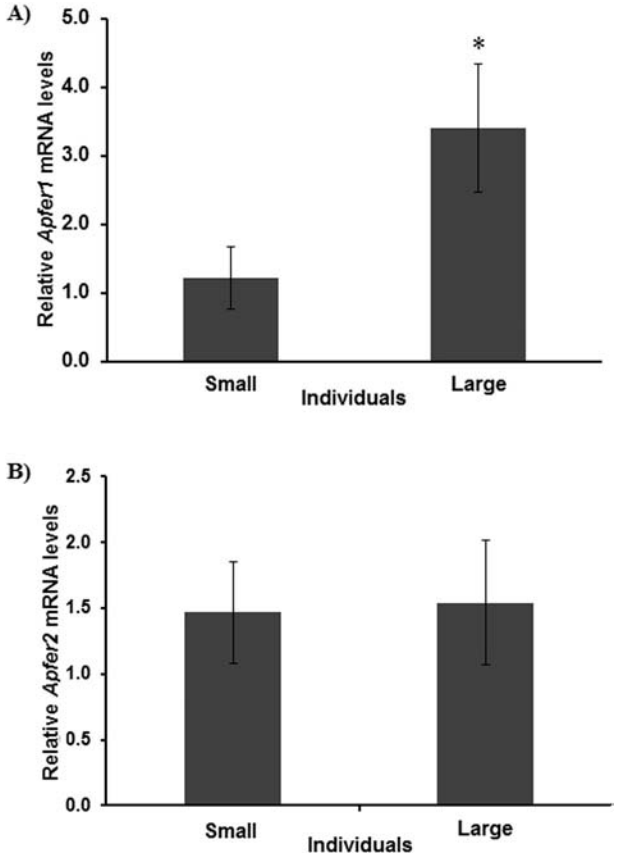


**Fig. 8.** Relative levels of *Apfer1* (A) and *Apfer2* (B) mRNA transcripts in mantle of slow-growing and fast-growing scallops. Slow-growing and fast-growing 4-month-old individuals (10.88 ± 0.65 and 25.25 ± 1.71 mm in shell height, respectively) belong to a single reproduction batch. All values represent the means ± S.E. (n = 5 biological replicates of 4 pooled individuals each). Asterisk denotes $P < 0.01$.

Other functional roles for ferritins during larval development cannot be excluded. Given that scallop larvae begin to feed at the D-veliger stage, then they could be more exposed to pathogens than during the trochophore stage. Therefore, the observed significant increase of *Apfer1* and *Apfer2* expressions in veligers and pediveligers may suggest an immunity-related role in these larval stages, as suggested for some ferritins of *C. gigas* (Huan et al., 2014).

### 3.4. Apfer1 and Apfer2 expression and growth rate

Iron is a regulator of cell growth and proliferation. In mammals, ferritins are regulated by hormones and growth factors, and they have been associated with the regulation of cellular proliferation and oncogenesis (Harrison and Arosio, 1996; Torti and Torti, 2002). In insects, a ferritin subunit has been suggested to be a mitogen promoting cell proliferation and growth of imaginal disc cells of *Drosophila* by maintaining iron homoeostasis and antagonizing starvation response (Li, 2010). Lucas (2007) observed a differential expression of ferritin and other genes in experiments of microarrays when comparing slow- and fast-growing individuals of *Haliotis asinina* abalone. It was also observed that higher ferritin copy number is associated with faster growth in the freshwater pearl mussel *Hyriopsis cumingii* (Bai et al., 2011).

Relative expression levels of *Apfer1* and *Apfer2* were determined in mantle samples of 4-month-old *A. purpuratus* scallops with contrasting growth rate. *Apfer1* expression was significantly higher (2.8-fold) in the mantle of large individuals than in the small ones (3.4 ± 0.93 and 1.2 ± 0.45, respectively) (Fig. 8A). Conversely, no significant differences in *Apfer2* expression were observed between fast- and slow-growing individuals (Fig. 8B).

Differences in amounts of *Apfer1* mRNA between fast- and slow-growing scallops could be associated to differences in the transcriptional rate or *Apfer1* mRNA turnover, but also to the existence of different copy number of the gene, and the presence of single nucleotide polymorphisms (SNPs). In fact, the presence of larger copy number of ferritin genes has been associated with fast growth in *H. cumingii* (Bai et al., 2011). SNPs have also been associated with differential ferritin expression in the snail *Concholepas concholepas* (Chávez-Mardones et al., 2013) and a similar association could occur in this case. Studies related to these aspects will be necessary to clarify the causes of *Apfer1* expression in fast- and slow-growing scallops, and to validate *Apfer1* as a candidate gene for fast growth in *A. purpuratus*.

### 3.5. Expression of Apfer1 and Apfer2 in response to bacterial challenge

*V. splendidus* and other bacteria have been associated with massive mortality in cultures of *A. purpuratus* in commercial hatcheries located in northern Chile (Riquelme et al., 1995; Rojas et al., 2015). Thus, it is of great interest to characterize the infection process and the immune response of this mollusc. Several studies suggest an equal involvement of ferritins in innate immune defence in invertebrates as in vertebrates as part of the iron-withholding strategy (Ong et al., 2006). To determine whether *Apfer1* and *Apfer2* expressions were induced by bacterial challenge, haemocytes from individuals challenged with a suspension of attenuated *V. splendidus* were collected over a period of 48 h of bacterial challenge, and relative expressions of both genes were evaluated. Expression level of non-injected individuals at 0 h time point was taken as the basal level (relative gene expression level = 1). No significant changes in *Apfer1* expression were observed in haemocytes from

scallops injected with sterile seawater during the course of the experiment (Fig. 9A). However, after the challenge with *V. splendidus*, *Apfer1* was found to be slightly but significantly up-regulated after 6 h, and strongly up-regulated after 24 h (17.2 ± 0.34); that was about eight-fold compared with that in the corresponding control group (2.17 ± 0.15), and declined afterwards (Fig. 9A). In the case of *Apfer2*, no significant changes in gene expression were observed in either individuals injected with sterile seawater or individuals challenged with *V. splendidus* during the course of the experiment (Fig. 9B).

Our results in *A. purpuratus* were similar to those observed in the closest ferritin homologues from *A. irradians*, *Aifer1* and *Aifer2*, respectively, upon challenge with *Vibrio alginoliticus*, except that *Aifer1* induction was faster, occurring 3 to 12 h after challenge (He et al., 2011). A possible explanation of the different responses of *Apfer1* and *Apfer2* to bacterial challenge is that they may be controlled by different transcription factors, as suggested for differential induction of ferritins from *A. irradians* (Li et al., 2012). Both ferritin homologues also displayed different IREs, which could involve different regulations at post-transcriptional level (Torti and Torti, 2002).

Although ferritin induction by bacterial challenge has also been observed in other bivalve molluscs such as *M. yessoensis* (Zhang et al., 2013a; Sun et al., 2014), *Ruditapes phillipinarum* (Kim et al., 2012), *Venerupis phillipinarum* (Zhang et al., 2013b) and *Mesodesma donacium* (Maldonado-Aguayo et al., 2015), the function of this protein in immune defence against infection remains little investigated in this group. For other marine invertebrates, it has been suggested that bacterial infection stimulates production of ferritins, which store host iron, preventing iron acquisition by bacteria and thereby inhibiting bacterial growth and proliferation (Ong et al., 2006). Iron catalyses the generation of free radicals formed from hydrogen peroxide via the Fenton reaction. Mammalian ferritins display a strong response to oxidant agents at transcriptional level owing to the presence of the antioxidant responsive element (ARE) in their promoter region (Recalcati et al., 2008; Arosio and Levi, 2010). It has also been suggested that mammalian ferritins protect against cell injury from ROS generated by neutrophils and macrophages during infection and inflammation (Koorts and Viljoen, 2011). This anti-inflammatory action of ferritin involves the inhibition of ROS production through iron sequestration, that is, an antioxidant activity of ferritin during LPS-induced ROS up-regulation (Fan et al., 2014). It is interesting to note that *E. coli* bacteria expressing the recombinant ferritin proteins *Aifer1* and *Aifer2* from *A. irradians* displayed higher tolerance to $H_2O_2$, an inducer of ROS formation, suggesting that *Aifer1* and *Aifer2* are involved in ROS scavenging (He et al., 2011). These results suggest that the induction of our *Apfer1* and other ferritins upon bacterial challenge could also be related to a putative antioxidant activity.

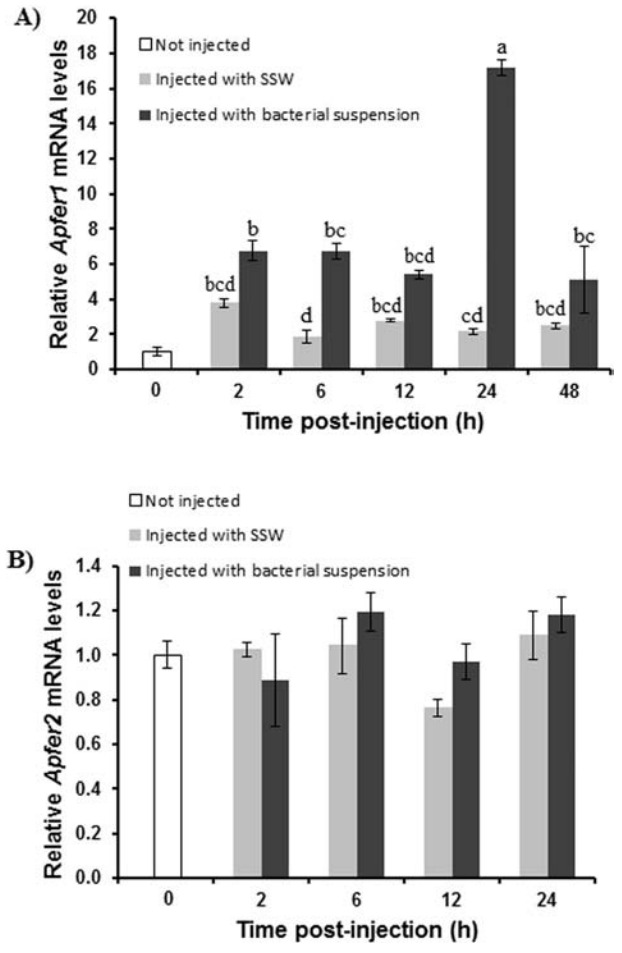


**Fig. 9.** mRNA transcript levels in haemocytes of *Argopecten purpuratus* after challenge with *Vibrio splendidus*. Time-course expression analyses of *Apfer1* (A) and *Apfer2* (B) transcript levels measured by quantitative RT-qPCR. Values corresponding to non-injected scallops (white bars), individuals injected with sterile saline water (SSW, grey bars) and individuals injected with bacterial suspension (dark grey bars) are displayed. Values are means ± SE (n = 5 biological replicates). Different letters denote $P < 0.05$.

## 4. Conclusions

In summary, two ferritin subunits (*Apfer1* and *Apfer2*) were isolated from *A. purpuratus*. They contained the typical elements of cytosolic ferritins and displayed high homology with two ferritins of *A. irradians*. Results suggested that both ferritins could be involved in larval development and shell formation. *Apfer1* expression level can be associated with growth rate and participate in the immune response against bacterial challenges. In turn, *Apfer2* did not show differences in expression rate between fast- and slow-growing scallops or in response to a bacterial challenge. These findings support ferritin *Apfer1* as a potential candidate gene to be used as a molecular marker for *A. purpuratus* growth and immune capacity enhancement through genetic programmes. Next step for this purpose will be to evaluate ferritin copy number in fast- and slow-growing individuals or individuals with contrasting performances at immune level, and to look for single nucleotide polymorphisms (SNPs) that could be involved in the differences of transcription rate. This information can be included in the estimation breeding values of potential brooders in a selective breeding programme. However, functional characterization experiments are required to verify the involvement of *Apfer1* in different physiological processes. One type of functional studies would be the characterization of this ferritin recombinant protein expressed in *E. coli* and the phenotype of transformed bacteria. Also, inhibition of *Apfer1* expressions by RNA interference would also allow the study of phenotypes of knock-down individuals.

## Acknowledgements

We would like to thank Germán Lira and William Farías for their technical support with animal maintenance. We also thank Roxana González and Fernando Jara for their assistance with laboratory analyses, and to Rodrigo Rojas who provides the bacterial strains. We thank Laboratorio Central de Cultivos Marinos of the UCN for providing the infrastructure for the experiments. This study was financed by the Fondo Nacional de Desarrollo Científico y Tecnológico (FONDECYT) of Chile, grants No 1130960 and 1140849 to FW and KB.

## References

Arosio, P., Levi, S., 2010. Cytosolic and mitochondrial ferritins in the regulation of cellular iron homeostasis and oxidative damage. Biochim. Biophys. Acta 1800, 783–792.
Arosio, P., Ingrassia, R., Cavadini, P., 2009. Ferritins: a family of molecules for iron storage, antioxidation and more. Biochim. Biophys. Acta 1790, 589–599.

Bai, Z., Yuan, Y., Yue, G., Li, J., 2011. Molecular cloning and copy number variation of a ferritin subunit (Fth1) and its association with growth in freshwater pearl mussel *Hyriopsis cumingii*. PLoS One 6, e22886.
Beck, G., Ellis, T.W., Habicht, G.S., Schluter, S.F., Marchalonis, J.J., 2002. Evolution of the acute phase response: iron release by echinoderm (*Asterias forbesi*) coelomocytes, and cloning of an echinoderm ferritin molecule. Dev. Comp. Immunol. 26, 11–26.
Boutet, I., Moraga, D., Marinovic, L., Obreque, J., Chavez-Crooker, P., 2008. Characterization of reproduction-specific genes in a marine bivalve mollusc: influence of maturation stage and sex on mRNA expression. Gene 407, 130–138.
Campillos, M., Cases, I., Hentze, M.W., Sanchez, M., 2010. SIREs: searching for iron-responsive elements. Nucleic Acids Res. 38, W360–W367.
Chávez-Mardones, J., Valenzuela-Muñoz, V., Núñez-Acuña, G., Maldonado-Aguayo, W., Gallardo-Escárate, C., 2013. *Concholepas concholepas* ferritin H-like subunit (*CcFer*): molecular characterization and single nucleotide polymorphism associated to innate immune response. Fish Shellfish Immunol. 35, 910–917.
Crichton, R.R., Declercq, J.P., 2010. X-ray structures of ferritins and related proteins. Biochim. Biophys. Acta 1800, 706–718.
De Zoysa, M., Lee, J., 2007. Two ferritin subunits from disk abalone (*Haliotis discus discus*): cloning, characterization and expression analysis. Fish Shellfish Immunol. 23, 624–635.
DiSalvo, L.H., Alarcón, E., Martínez, E., Uribe, E., 1984. Progress in mass culture of *Chlamys* (*Argopecten*) *purpurata* Lamarck (1819) with notes on its natural history. Rev. Chil. Hist. Nat. 57, 35–45.
Dunkov, B.C., Georgieva, T., 2004. Organization of the ferritin genes in *Drosophila melanogaster*. DNA Cell Biol. 18, 937–944.
Durand, J.P., Goudard, F., Pieri, J., Escoubas, J.M., Schreider, N., Cadoret, J.P., 2004. *Crassostrea gigas* Ferritin: cDNA sequence analysis for two heavy chain type subunits and protein purification. Gene 338, 187–195.
Fan, Y., Zhang, J., Cai, L., Wang, S., Liu, C., Zhang, Y., You, L., Fu, Y., Shi, Z., Yin, Z., Luo, L., Chang, Y., Duan, X., 2014. The effect of anti-inflamatory properties of ferritin light chain on lipopolysaccharide-induced inflammatory response in murine macrophages. Biochim. Biophys. Acta 1843, 2775–2783.
Finazzi, D., Arosio, P., 2014. Biology of ferritin in mammals: an update on iron storage, oxidative damage and neurodegeneration. Arch. Toxicol. 88, 1787–1802.
Galatro, A., Puntarulo, S., 2007. Mitochondrial ferritin in animals and plants. Front. Biosci. 12, 1063–1071.
Giorgi, A., Mignogna, G., Bellapadrona, G., Gattoni, M., Chiaraluce, R., Consalvi, V., Chiancone, E., Stefanini, S., 2008. The unusual co-assembly of H- and M-chains in the ferritin molecule from the Antartic teleosts *Trematomus bernachii* and *Trematomus newnesi*. Arch. Biochem. Biophys. 478, 69–74.
Harrison, P.M., Arosio, P., 1996. The ferritins: molecular properties, iron storage function and cellular regulation. Biochim. Biophys. Acta 1275, 161–203.
He, X., Zhang, Y., Wu, X., Xiao, S., Yu, Z., 2011. Cloning and characterization of two ferritin subunit genes from bay scallop, *Argopecten irradians* (Lamarck 1819). Mol. Biol. Rep. 38, 2125–2132.
Huan, P., Liu, G., Wang, H., Liu, B., 2014. Multiple ferritin subunit genes of the Pacific oyster *Crassostrea gigas* and their distinct expression patterns during early development. Gene 546, 80–88.
Kim, H., Elvitigala, D.A.S., Lee, Y., Lee, S., Whang, I., Lee, J., 2012. Ferritin H-like subunit from Manila clam (*Ruditapes philippinarum*): molecular insights as a potent player in host antibacterial defense. Fish Shellfish Immunol. 33, 926–936.
Koorts, A.M., Viljoen, M., 2011. Acute Phase Proteins: Ferritin and Ferritin Isoforms. In: Veas, F. (Ed.), Acute Phase Proteins — Regulation and Functions of Acute Phase. InTech, Sanghai, pp. 153–184.
Laurell, H., Iacovoni, J.S., Abot, A., Svec, D., Maoret, J.-J., Arnal, J.-F., Kubista, M., 2012. Correction of RT–qPCR data for genomic DNA-derived signals with ValidPrime. Nucleic Acids Res. 40, e51.
Le Brun, N.E., Crow, A., Murphy, M.E., Mauk, A.G., Moore, G.R., 2010. Iron core mineralization in prokaryotic ferritins. Biochim. Biophys. Acta 1800, 732–744.
Li, J., Li, L., Zhang, S., Li, J., Zhang, G., 2012. Three ferritin subunits involved in immune defense from bay scallop *Argopecten irradians*. Fish Shellfish Immunol. 32, 368–372.
Li, S., 2010. Identification of iron-loaded ferritin as an essential mitogen for cell proliferation and postembryonic development in *Drosophila*. Cell Res. 20, 1148–1157.
Liu, X., Theil, E.C., 2005. Ferritins: dynamic management of biological iron and oxygen chemistry. Acc. Chem. Res. 38, 167–175.
Liu, X., Hintze, K., Lonnerdal, B., Theil, E.C., 2006. Iron at the center of ferritin, metal/oxygen homeostasis and novel dietary strategies. Biol. Res. 39, 167–171.
Lucas, T., 2007. Investigating Genetic and Molecular Aspects of Growth of the Tropical Abalone *Haliotis asinina* (PhD Thesis) University of Queensland.
Maldonado-Aguayo, W., Lafarga-De la Cruz, F., Gallardo-Escárate, C., 2015. Identification and expression of antioxidant and immune defense genes in the surf clam *Mesodesma donacium* challenged with *Vibrio anguillarum*. Mar. Biol. 19, 65–73.
Marigómez, I., Soto, M., Cajaraville, M.P., Angulo, E., Giamberini, L., 2002. Cellular and subcellular distribution of metals in mollusks. Microsc. Res. Tech. 56, 358–392.
Marin, F., Luquet, G., Marie, B., Medakovic, D., 2008. Molluscan shell proteins: primary structure, origin, and evolution. Curr. Top. Dev. Biol. 80, 209–276.
Ong, S.T., Ho, J.Z., Ho, B., Ding, J.L., 2006. Iron-withholding strategy in innate immunity. Immunobiology 211, 295–314.
Pérez, H.M., Brokordt, K.B., Martínez, G., Guderley, H., 2009. Locomotion versus spawning: escape responses during and after spawing in the scallop *Argopecten purpuratus*. Mar. Biol. 156, 1585–1593.
Pfaffl, M.W., 2001. A new mathematical model for relative quantification in real-time RT-PCR. Nucleic Acids Res. 29, 2002–2007.
Pham, D.Q., Winzerling, J.J., 2010. Insect ferritins: typical or atypical? Biochim. Biophys. Acta 1800, 824–833.
Piccninelli, P., Samuelsson, T., 2007. Evolution of the iron-responsive element. RNA 13, 952–966.
Recalcati, S., Invernizzi, P., Arosio, P., Cairo, G., 2008. New functions for an iron storage protein: the role of ferritin in immunity and autoimmunity. J. Autoimmun. 30, 84–89.
Riquelme, C., Hayashida, G., Vergara, N., Vásquez, A., Morales, Y., Chávez, P., 1995. Bacteriology of the scallop *Argopecten purpuratus* (Lamarck, 1819) cultured in Chile. Aquaculture 138, 49–60.
Rojas, R., Miranda, C.D., Opazo, R., Romero, J., 2015. Characterization and pathogenicity of *Vibrio splendidus* strains associated with massive mortalities of commercial hatchery-reared larvae of scallop *Argopecten purpuratus* (Lamarck, 1819). J. Invertebr. Pathol. 124, 61–69.
Saitou, N., Nei, M., 1987. The neighbor-joining method: a new method for reconstructing phylogenetic trees. Mol. Biol. Evol. 4, 406–425.
Salinas-Clarot, K., Gutiérrez, A.P., Núñez-Acuña, G., Gallardo-Escárate, C., 2011. Molecular characterization and gene expression of ferritin in red abalone (*Haliotis rufescens*). Fish Shellfish Immunol. 30, 430–433.
SAS Institute, 1999. The SAS System for Windows. Release 8.0. SAS Institute, North Carolina.
Schrödinger, L.L.C., 2010. The PyMOL Molecular Graphics System, Version 1.3r1. Schrödinger, L.L.C., Portland, Oregon.
Simonsen, K.T., Møller-Jensen, J., Kristensen, A.R., Andersen, J.S., Riddle, D.L., Kallipolitis, B.H., 2011. Quantitative proteomics identifies ferritin in the innate immune response of *C. elegans*. Virulence 2, 120–130.
Snedecor, G., Cochran, W., 1989. Statistical Methods. eighth ed. Iowa State University Press, Iowa.
Stotz, W.B., González, S.A., 1997. Abundance, growth, and production of the sea scallop *Argopecten prupuratus* (Lamarck 1819): bases for sustainable exploitation of natural scallop beds in north-Central Chile. Fish. Res. 32, 173–183.
Sun, Y., Zhang, Y., Fu, X., Zhang, R., Zou, J., Wang, S., Hu, X., Zhang, L., Bao, Z., 2014. Identification of two secreted ferritin subunits involved in immune defense of Yesso scallop *Patinopecten yessoensis*. Fish Shellfish Immunol. 37, 53–59.
Tamura, K., Nei, M., Kumar, S., 2004. Prospects for inferring very large phylogenies by using the neighbor-joining method. Proc. Natl. Acad. Sci. U. S. A. 101, 11030–11035.
Tamura, K., Stecher, G., Peterson, D., Filipski, A., Kumar, S., 2013. MEGA6: molecular evolutionary genetics analysis version 6.0. Mol. Biol. Evol. 30, 2725–2729.
Theil, E.C., 1987. Ferritin: structure, gene regulation and cellular functions in animals, plants and microorganisms. Annu. Rev. Biochem. 56, 289–315.
Theil, E.C., 1994. Iron regulatory elements (IREs): a family of mRNA non-coding sequences. Biochem. J. 304, 1–11.
Theil, E.C., 2015. IRE mRNA riboregulators use metabolic iron ($Fe^{2+}$) to control mRNA activity and iron chemistry in animals. Metallomics 7, 15–24.
Torti, F.M., Torti, S.V., 2002. Regulation of ferritin genes and protein. Blood 99, 3505–3516.
Wang, X., Liu, B., Xiang, J., 2009. Cloning, characterization and expression of ferritin subunit from clam *Meretrix meretrix* in different larval stages. Comp. Biochem. Physiol. B 154, 12–16.
Wu, C., Zhang, W., Mai, K., Xu, W., Wang, X., Ma, H., Liufu, Z., 2010. Transcriptional up-regulation of a novel ferritin homolog in abalone *Haliotis discus hannai* by dietary iron. Comp. Biochem. Physiol. C 152, 424–432.
Xie, J., Cao, X., Wu, L., Luo, M., Zhu, Z., Huang, Y., Wu, X., 2012. Molecular and functional characterization of ferritin in abalone *Haliotis diversicolor supertexta*. Acta Oceanol. Sin. 31, 87–97.
Zapata, M., Tanguy, A., David, E., Moraga, D., Riquelme, C., 2009. Transcriptomic response of *Argopecten purpuratus* post-larvae to copper exposure under experimental conditions. Gene 442, 37–46.
Zhang, L., Sun, W., Cai, W., Zhang, Z., Gu, Y., Chen, H., Ma, S., Jia, X., 2013b. Differential response of two ferritin subunit genes (*VpFer1* and *VpFer2*) from *Venerupis philippinarum* following pathogen and heavy metals challenge. Fish Shellfish Immunol. 35, 1658–1662.
Zhang, Y., 2008. I-TASSER server for protein 3D structure prediction. BMC Bioinf. 9, 40.
Zhang, Y., Meng, Q., Jiang, T., Wang, H., Xie, L., Zhang, R., 2003. A novel ferritin subunit involved in shell formation from the pearl oyster (*Pinctada fucata*). Comp. Biochem. Physiol. B 135, 43–54.
Zhang, Y., Zhang, R., Zou, J., Hu, X., Wang, S., Zhang, L., Bao, Z., 2013a. Identification and characterization of four ferritin subunits involved in immune defense of the Yesso scallop (*Patinopecten yessoensis*). Fish Shellfish Immunol. 34, 1178–1187.